Source and Ground Motion Models for Australian Earthquakes

Paul Somerville[1,2], Robert Graves[1], Nancy Collins[1], Seok Goo Song,[1] and Sidao Ni[1] and Phil Cummins[3]

1. URS Corporation, Pasadena, California

2. Risk Frontiers, Macquarie University

3. Geoscience Australia

Abstract

We have developed models for the prediction of ground motion response spectra in several regions of Australia for rock site conditions (V_s30 of 865 m/sec). In Eastern Australia, we developed models for the Paleozoic Lachlan Fold Belt, and the Sydney Basin that lies within it, and in Western Australia we developed models for the Yilgarn Craton and the adjacent Perth Basin. The models are based on the broadband simulation of accelerograms using regional crustal velocity models and earthquake source scaling relations. For both the Lachlan Fold Belt and Yilgarn regions, we used comparison of synthetic seismograms with the recorded seismograms of small earthquakes to test and modify regional crustal velocity models. In Western Australia, we used the rupture models of the 1968 M_w 6.6 Meckering earthquake and the 1988 M_w 6.25, 6.4 and 6.6 Tennant Creek earthquakes to constrain the scaling relationship between seismic moment and rupture area. Other aspects of the source scaling relations were derived from our scaling relations for earthquakes in eastern North America (Somerville et al., 2001). In eastern Australia, the data available for historical earthquakes are insufficient to constrain earthquake scaling relations, so we have used the relations for Western Australia as well as the relations for the western United States (Somerville et al., 1999). We generated suites of broadband ground motion time histories using these source scaling relations and crustal structure models. These ground motion simulations were used to generate ground motion prediction models for each region. These models were distilled into two separate models: one for cratonic and the other for non-cratonic regions of Australia. The ground motion models are compared with the model of Liang et al. (2008) for Western Australia, with models for Eastern North America including Atkinson and Boore (2006), Somerville et al (2001), and Toro et al (1997), and with the NGA models. The models are also compared with ground motions recorded in Australia.

Key Words: Earthquake source, earthquake ground motions.

INTRODUCTION

This paper describes source and ground motion prediction models for Australian earthquakes. Given the sparsity of recorded strong motion data in Australia, we used a broadband strong motion simulation procedure that can account for the known earthquake source and crustal structure properties of this region. The strong motion simulations used earthquake source scaling relations that are consistent with the source parameters that we derived from large Australian earthquakes, and Green's functions that are calculated from validated crustal structure models of Australia. This work, described in more detail in Somerville et al. (2009), builds on previous work by Trevor Allen and his co-authors listed in the References.

CRUSTAL STRUCTURE MODELS

Crustal structure models for the Perth Basin/Yilgarn Craton in southwestern Australia and the Sydney Basin/Lachlan Fold Belt were investigated by reviewing the work of Collins et al. (2003) and modeling teleseismic receiver functions, short period surface wave dispersion and local waveforms. We determined crustal thickness and V_p/V_s (ratio of P to S wave velocity) for selected regions by applying an *h-k* stacking algorithm. For the Perth Basin/Yilgarn Craton area, the Moho is about 36 km deep and V_p/V_s is about 1.73. For the Sydney Basin /Lachlan Fold Belt, the Moho is about 40 km deep and V_p/V_s is about 1.75. With V_p/V_s resolved, S wave velocity profiles were approximated based on P wave velocity profiles from various seismic refraction/reflection studies.

For the Yilgarn Craton, we took advantage of abundant shallow seismicity in the southwest seismic zone (SWSZ) which excites strong short period Rayleigh waves (R_g), and we used surface wave dispersion (0.5s-5s) to constrain the shallow structure of this region. A 1 km thick low velocity zone (V_s 3.15km/s) overlying crystalline basement (Vs ~3.5km/s) is required to explain the strongly dispersed R_g wave. By modeling the details of receiver functions, we found that the mid-crustal discontinuity is shallower than indicated in previous studies, i.e., at a depth of 12-15km instead of 20-25km. Also, the Moho seems to be fairly sharp. We also resolved the source mechanism and depth of the 2007/10/09 Katanning M_w 4.7 earthquake, whose M_w value was obtained from long period waves in this study, and, which is the largest earthquake in that region for 40 years. This event is also very shallow (depth <3km) with a mostly dip-slip mechanism with some strike slip, consistent with other major earthquakes in the Yilgarn Craton.

For the Sydney/Lachlan Fold Belt, we studied broadband waveforms of the 2003/12/11 M_w 3.8 Moss Vale earthquake, whose Mw value was obtained from long period waves in this study. We constructed synthetic seismograms based on a V_p model from seismic refraction and a V_s model from teleseismic modeling of V_p/V_s. By modeling the sP_mP phase, we were able to determine the focal depth to be 6-8 km.

Based on measurements of shear wave velocities at shallow depths at rock sites in Australia (Collins et al., 2006), we selected a V_s30 value of 865 m/sec to represent rock sites in conditions in all of the crustal structure models that we used for ground motion simulations, and so the ground motion prediction models presented below are for those conditions.

EARTHQUAKE SOURCE MODELS

We generated finite fault rupture models of large Australian earthquakes, specifically the 1968 Meckering and 1988 Tennant Creek earthquakes (Table 1). The rupture models were derived through the inversion of teleseismic waves, and, in the case of the Meckering earthquake, geodetic and surface faulting data. Finite fault rupture models have not previously been derived from any Australian earthquakes, although analyses of surface geology and teleseismic waves have been used to infer the extent of the fault ruptures that generated these earthquakes. We used the rupture models of these earthquakes and other data to derive earthquake source models for use in strong motion simulations. The scaling relation for rupture area used to represent the cratonic Australian earthquakes was chosen to be consistent with the largest earthquake of the Tennant Creek sequence and with the Meckering earthquake (Figure 1), and is given by:

$$\mathrm{Log}_{10}\, A = 2/3 \log M_o - 14.95$$

where A = rupture area in sq km and M_o is seismic moment in dyne.com. This scaling relation has a rupture area that is half that of earthquakes in the tectonically active Western North America. This is similar to a scaling relation for Stable Continental Region (SCR) earthquakes developed by Leonard (2008). The scaling of the cratonic Australian earthquakes is compared with that of earthquakes in eastern North America in Figure 1, which also shows estimates of the seismic moment and rupture areas of three small eastern Canadian earthquakes that were derived from rupture model inversions (Hartzell et al., 1994); the three New Madrid earthquakes of 1811 – 1812 (Petersen et al., 2008); and the 1886 Charleston earthquake in the eastern United States.

For non-cratonic Australia, we do not have large enough earthquakes to derive finite fault rupture models, so the scaling relations of these earthquakes are uncertain. Accordingly, we used two scaling relations. The first assumes that the scaling relations of earthquakes are the same as those in Western North America. The second assumes that the scaling relations of earthquakes are the same as those in cratonic Australia.

Table 1. Fault Parameters of Cratonic Australian Earthquakes

Event	M_o x 10^{25} dyne.cm	M_w	L km	W km	A km^2
Meckering	8.2	6.6	25	7	280
Tennant Creek #1	2.7	6.25	12	16	192
Tennant Creek #2	3.5	6.4	16	10	160
Tennant Creek #3	9.2	6.6	18	12	216

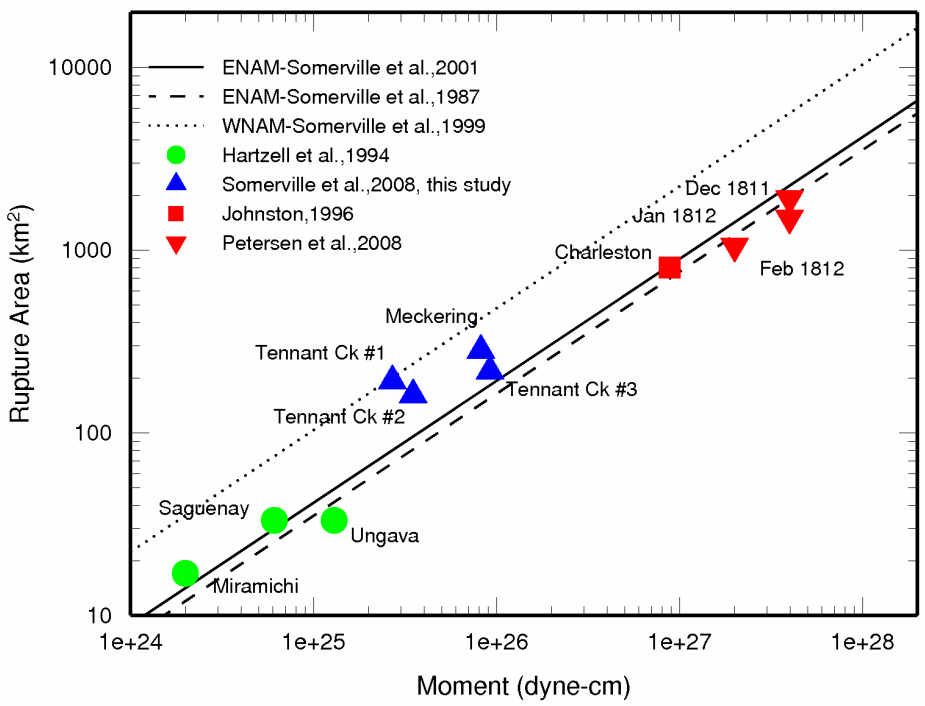

Figure 1. Seismic moment and rupture areas of cratonic Australian earthquakes, and comparison with data from Eastern North America and with several scaling relations.

GROUND MOTION MODELS

Ground motions were simulated using the hybrid method of Graves and Pitarka (2004) and Graves et al. (2007), in which ground motions are computed separately in the high frequency and low frequency ranges, and then combined into a single broadband time history using matched filters. For low frequencies (below 1 Hz), we use complete theoretical seismograms, whereas for high frequencies (above 1 Hz) we use a simpler stochastic approach based on Boore (1983). Ground motions were simulated for magnitudes from M_w 5 to 7.5 for six combinations of earthquake source and crustal structure. One of these consisted of the cratonic source model and the Yilgarn Craton crustal structure. The other five consisted of the cratonic source model in the Perth Basin, and both the cratonic and non-cratonic source models in both the Lachlan Fold Belt and the Sydney Basin crustal structure models. The Yilgarn Craton ground motion model is quite different from the other five models, which are all quite similar to each other.

The similarity in ground motions obtained in the same crustal structure using the two different source models is attributable to a trade-off between the effects of the different source dimensions and rise times. The cratonic earthquake source models have rupture areas that are half those of the non-cratonic source models, which causes them to have higher ground motions. However, the cratonic earthquake source models also have rise times that are 1.86 times longer than those of the non-cratonic source models, equivalent to a subfault corner frequency scaling factor that is 1.86 times lower, which causes them to have lower ground motions. These two source effects approximately offset each other for all distances and magnitudes. Using a stochastic ground motion simulation model, Risk Engineering Inc. (2001) similarly found that, except for the effects of differences in kappa, the ground motions for eastern North America (cratonic model) and western North America (non-cratonic model) are similar for a given reference site condition. Accordingly, we developed a model for non-cratonic Australia by combining the ground motion simulations of the five non-cratonic cases whose ground motion models we found to be similar. The crustal structures contained in the non-cratonic model, which include the Lachlan Fold Belt, the Sydney Basin, and the Perth Basin, are considered to be representative of non-cratonic Australia, especially its coastal margins. Both the cratonic and non-cratonic earthquake source models were used in conjunction with the Lachlan Fold Belt and Sydney Basin, while only the cratonic source model was used in conjunction with the Perth Basin. Thus the relative weighs of the cratonic and non-cratonic source models in the combined non-cratonic ground motion model are 60% and 40% respectively. It is considered that the Yilgarn Craton model is, to first order, applicable to the Yilgarn Craton and other cratonic regions of Australia. It is considered that the non-cratonic model is, to first order, applicable in all non-cratonic regions of Australia. In particular, it is considered to be applicable to non-cratonic coastal regions, including all of the state capitals of Australia. The parameters of these two ground motion models are given in Tables 2, 3 and 4.

The cratonic ground motion model is quite similar to the model developed using Yilgarn Craton data by Liang et al. (2008) model, and less similar to the models for stable regions of eastern North America by Toro et al (1997) and Atkinson and Boore (2006), as shown on the left side of Figure 2. The very large ground motions predicted by the cratonic model at periods of 1 second and longer are due to surface waves that are generated by shallow faulting and trapped in a shallow layer (1 km thick) of lower velocity rock; such waves are prominently recorded in the Yilgarn craton. The non-cratonic ground motion

model is more similar to models for tectonically active regions such as Boore and Atkinson (2008) than the Toro et al. (1997) model for tectonically stable eastern North America, as shown on the right side of Figure 2, mainly due to the higher value of kappa used in the non-cratonic model than in Toro et al. (1997). We used kappa values of 0.006 and 0.04 respectively with the cratonic and non-cratonic models.

The predictions of the non-cratonic ground motion model were compared with ground motion recordings of the Mw 4.47 Thomson Reservoir earthquake of 26 September 1996 (Allen et al., 2000) that occurred about 135 km east of Melbourne (Figure 3). This earthquake has a large number of recordings that span the distance range of interest. The ground motion model was developed from simulations in the magnitude range of 5.0 to 7.5, so its use for a magnitude 4.47 earthquake involves some extrapolation. The shape of the decrease in predicted ground motion levels with distance is generally consistent with that of the data. The flattening in slope that occurs at 50 km in the model is consistent with a flattening that is evident in the data, especially at periods of 1 second and longer. In general, the level of the model predictions is consistent with that of the data, although the model tends to overpredict the data for periods of 0.2 to 0.4 seconds. Overall, the agreement between the model and the recorded data of this earthquake is quite good.

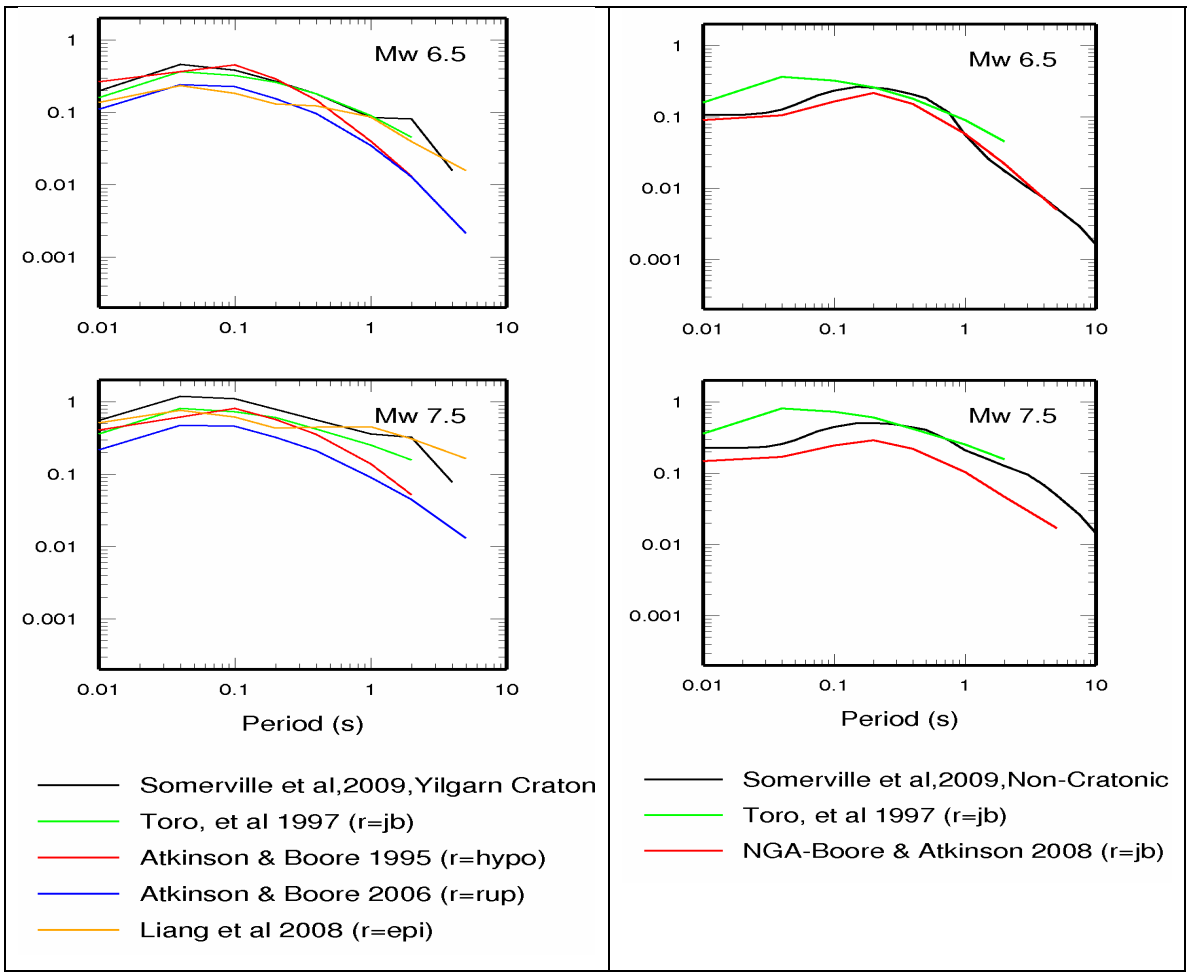

Figure 2. Comparison of cratonic model response spectrum (blackline, left) and non-cratonic model response spectrum (black line, right) with other ground motion models for magnitude 6.5 and 7.5 earthquakes at a distance of 30 km. The vertical axis shows response spectral acceleration in g's as a function of period on the horizontal axis.

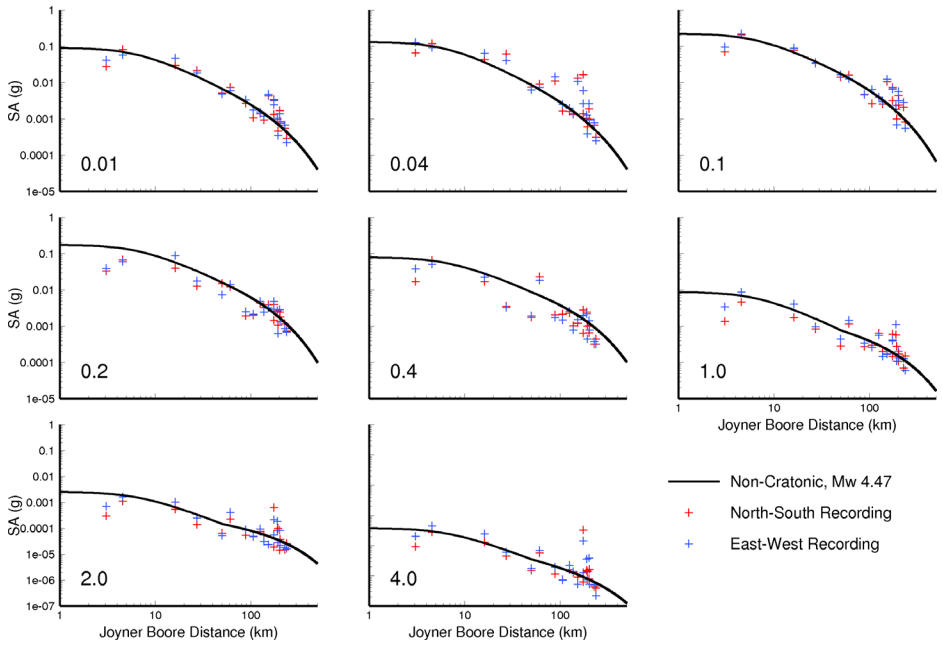

Figure 3. Comparison of recorded spectral accelerations of the September 25, 1996 Thompson Reservoir earthquake with the predictions of the non-cratonic model. The vertical axis shows response spectral acceleration in g's as a function of distance on the horizontal axis, for periods from 0.01 sec (PGA) to 4.0 sec.

Table 2. Form of the Ground Motion Models

for $M < m_1$, $r < r_1$

$$\ln Sa(g) = c_1 + c_2(M - m_1) + c_3 \ln R + c_4(M - m_1) \ln R + c_5 r + c_8(8.5 - M)^2$$

for $M < m_1$, $r \geq r_1$

$$\ln Sa(g) = c_1 + c_2(M - m_1) + c_3 \ln R_1 + c_4(M - m_1) \ln R + c_5 r + c_6(\ln R - \ln R_1) + c_8(8.5 - M)^2$$

for $M \geq m_1$, $r < r_1$

$$\ln Sa(g) = c_1 + c_7(M - m_1) + c_3 \ln R + c_4(M - m_1) \ln R + c_5 r + c_8(8.5 - M)^2$$

for $M \geq m_1$, $r \geq r_1$

$$\ln Sa(g) = c_1 + c_7(M - m_1) + c_3 \ln R_1 + c_4(M - m_1) \ln R + c_5 r + c_6(\ln R - \ln R_1) + c_8(8.5 - M)^2$$

where

Sa(g)	is spectral acceleration in g for rock sites having V_s30 of 865 m/sec
m_1	= 6.4
r_1	= 50 km
h	= 6 km
R	$= \sqrt{r^2 + h^2}$
R_1	$= \sqrt{r_1^2 + h^2}$
M	is moment magnitude in the range of 5.0 to 7.5
r	= Joyner Boore distance in the range of 0 to 500 km

Table 3. Ground Motion Model for Non-Cratonic Australia

Period	C1	C2	C3	C4	C5	C6	C7	C8	σ
PGA	1.03780	-0.03970	-0.79430	0.14450	-0.00618	-0.72540	-0.03590	-0.09730	0.5685
0.010	1.05360	-0.04190	-0.79390	0.14450	-0.00619	-0.72660	-0.03940	-0.09740	0.5684
0.020	1.05680	-0.03920	-0.79680	0.14550	-0.00617	-0.73230	-0.03930	-0.09600	0.5684
0.030	1.13530	-0.04790	-0.80920	0.15000	-0.00610	-0.76410	-0.05710	-0.09210	0.5681
0.040	1.30000	-0.07020	-0.83150	0.15920	-0.00599	-0.82850	-0.09810	-0.08530	0.5676
0.050	1.47680	-0.09310	-0.83330	0.15600	-0.00606	-0.86740	-0.12740	-0.09130	0.5670
0.075	1.70220	-0.05160	-0.80720	0.14560	-0.00655	-0.87690	-0.10970	-0.08690	0.5663
0.100	1.65720	0.15080	-0.77590	0.13100	-0.00708	-0.77830	0.01690	-0.05980	0.5659
0.150	1.94440	-0.09620	-0.75000	0.11670	-0.00698	-0.69490	-0.13320	-0.12530	0.5659
0.200	1.82720	-0.06230	-0.73430	0.11940	-0.00677	-0.64380	-0.09570	-0.11920	0.5669
0.250	1.74380	-0.02530	-0.72480	0.11950	-0.00646	-0.63740	-0.06250	-0.11650	0.5678
0.3003	1.80560	-0.27020	-0.73190	0.13490	-0.00606	-0.66440	-0.17470	-0.14340	0.5708
0.400	1.88750	-0.37820	-0.70580	0.09960	-0.00589	-0.58770	-0.24420	-0.21890	0.5697
0.500	2.03760	-0.79590	-0.69730	0.11470	-0.00565	-0.59990	-0.48670	-0.29690	0.5739
0.750	1.93060	-0.80280	-0.74510	0.11220	-0.00503	-0.59460	-0.50120	-0.34990	0.5876
1.000	1.60380	-0.47800	-0.86950	0.07320	-0.00569	-0.41590	0.06360	-0.33730	0.6269
1.4993	0.47740	0.90960	-1.02440	0.11060	-0.00652	-0.19000	1.09610	-0.10660	0.7517
2.000	-0.25810	1.37770	-1.01000	0.10310	-0.00539	-0.27340	1.50330	-0.04530	0.8036
3.0003	-0.96360	1.14690	-0.88530	0.10380	-0.00478	-0.40420	1.54130	-0.11020	0.8219
4.000	-1.46140	1.07950	-0.80490	0.10960	-0.00395	-0.46040	1.41960	-0.14700	0.8212
5.000	-1.61160	0.74860	-0.78100	0.09650	-0.00307	-0.46490	1.24090	-0.22170	0.8240
7.5019	-2.35310	0.35190	-0.64340	0.09590	-0.00138	-0.68260	0.92880	-0.31230	0.7957
10.000	-3.26140	0.69730	-0.62760	0.12920	-0.00155	-0.61980	1.01050	-0.24550	0.7602
PGV	5.07090	0.52780	-0.85740	0.17700	-0.00501	-0.61190	0.80660	-0.03800	0.6417

Table 4. Ground Motion Model the Yilgarn Craton, Australia

Period	C1	C2	C3	C4	C5	C6	C7	C8	σ
PGA	1.54560	1.45650	-1.11510	0.16640	-0.00567	-1.04900	1.05530	0.20000	0.5513
0.010	1.55510	1.46380	-1.11460	0.16620	-0.00568	-1.04840	1.05850	0.20140	0.5512
0.020	2.33800	1.38060	-1.22970	0.18010	-0.00467	-1.39850	0.95990	0.20130	0.5510
0.030	2.48090	1.37540	-1.17620	0.17120	-0.00542	-1.38720	0.96930	0.19280	0.5508
0.040	2.31450	1.60250	-1.12600	0.17150	-0.00629	-1.27910	1.07040	0.23560	0.5509
0.050	2.26860	1.55840	-1.07340	0.14710	-0.00709	-1.08910	1.10750	0.20670	0.5510
0.075	1.97070	1.68030	-1.01540	0.14560	-0.00737	-0.91930	1.18290	0.22170	0.5514
0.100	1.71030	1.75070	-0.99330	0.13820	-0.00746	-0.78140	1.29390	0.23790	0.5529
0.150	1.52310	1.69160	-0.96310	0.13330	-0.00713	-0.67330	1.22430	0.21020	0.5544
0.200	1.36830	1.57940	-0.94720	0.13640	-0.00677	-0.62690	1.17760	0.18950	0.5558
0.250	1.40180	1.28940	-0.94410	0.14360	-0.00617	-0.67070	1.05610	0.14590	0.5583
0.3003	1.45000	1.04630	-0.94880	0.14760	-0.00581	-0.68700	0.94040	0.11040	0.5602
0.400	1.44150	0.92820	-0.91830	0.11320	-0.00576	-0.59520	0.86280	0.04060	0.5614
0.500	1.40380	0.69160	-0.91010	0.13480	-0.00557	-0.62390	0.71230	0.00620	0.5636
0.750	1.50840	0.75800	-0.99010	0.11260	-0.00458	-0.69040	0.68590	-0.05630	0.5878
1.000	2.10630	0.38180	-1.08680	0.07950	-0.00406	-0.90340	0.61850	-0.18250	0.6817
1.4993	2.55790	-0.84270	-0.81810	0.07650	-0.00220	-1.35320	-0.25440	-0.46660	0.8514
2.000	2.39600	-1.39950	-0.70440	0.06770	-0.00366	-0.90860	-0.64320	-0.59600	0.8646
3.0003	0.96040	-0.46120	-0.70450	0.06450	-0.00429	-0.51190	-0.16430	-0.46310	0.8424
4.000	0.12190	-0.06980	-0.75910	0.08490	-0.00374	-0.41450	0.12350	-0.39250	0.8225
5.000	-0.84240	0.53160	-0.79600	0.10330	-0.00180	-0.62130	0.53680	-0.27570	0.8088
7.5019	-1.92260	0.63760	-0.81900	0.14550	-0.00066	-0.75740	0.69020	-0.23290	0.7808
10.000	-2.60330	0.59060	-0.80940	0.16090	-0.00106	-0.68550	0.70350	-0.22910	0.7624
PGV	5.23440	1.58530	-1.01540	0.21400	-0.00341	-0.91610	1.12980	0.14810	0.6606

ACKNOWLEDGMENTS

This paper describes work done by URS under contract to Geoscience Australia. The authors would like to acknowledge the many contributions of Trevor Allen to this study, including the estimates of kappa that he provided, and the review comments of Gary Gibson. The ground motion data shown in Figure 2 come from a database of Australian strong ground motions that was assembled in a collaborative effort between Geoscience Australia, Environmental Systems and Services (ES&S), and the Australian National Committee on Large Dams (ANCOLD), with a large proportion of the strong motion data being supplied by ES&S. This strong motion data base forms the principal data source

available for the development of ground motion prediction models in Australia.

REFERENCES

Allen, T. and G.M. Atkinson (2006). Comparison of earthquake source spectra and attenuation in southeastern Australia and eastern North America. Proceedings of the 2006 Conference of the Australian Earthquake Engineering Society, p. 63-67, Canberra, ACT.

Allen, T.I., P.R. Cummins, T. Dhu and J.F. Schneider (2006b). Attenuation of ground motion spectral amplitudes in southeastern Australia. Bull. Seism. Soc. Am. 96, 572-585.

Allen, T.I., T. Dhu, P.R. Cummins, and J.F. Schneider (2006a). Empirical attenuation of ground motion spectral amplitudes in southwestern Western Australia. Bull. Seism. Soc. Am. 96, 572-585, April, doi: 10.1785/0120040238.

Allen, T.I., G. Gibson, A. Brown, and J.P. Cull (2004). Depth variation of seismic source scaling relations: implications for earthquake hazard in southeast Australia. Tectonophysics 390, 5-4.

Allen, T.I., G. Gibson and C. Hill (2000). The Thompson Reservoir triggered earthquakes. Proceedings of the 2000 Conference of the Australian Earthquake Engineering Society.

Atkinson, G.M. and Boore, D.M. (2006). Earthquake ground-motion prediction equations for eastern North America. *Bull. Seism. Soc. Am.*, 96, 2181-2205.

Atkinson. G.M and D.M. Boore (1996). New ground motion relations for eastern North America. *Bull. Seism. Soc. Am*. 85, 17-30.

Boore, D.M. (1983). Stochastic simulation of high-frequency ground motions based on seismological models of the radiated spectra. *Bull. Seism. Soc. Am.*, **73**, 1865–1894.

Boore, David M., and Gail M. Atkinson (2008). Ground motion prediction equations for the average horizontal component of PGA, PGV and 5% damped PSA at spectral periods between 0.01s and 10.0s. *Earthquake Spectra* 24, 99-138.

Collins C, R. Kayen, B. Carkin, T. Allen, P. Cummins and A. McPherson (2006). Shear Wave Velocity measurement at Australian Ground Motion Seismometer Sites by the Spectral Analysis of Surface Waves (SASW) Method, GA report 10008.

Collins, C.D.N., B.J. Drummond, and M.G. Nicoll (2003). Crustal structure thickness patterns in the Australian continent. Geol. Soc. Australia Spec. Pub. 22, 121-128.

Graves, R. W. and A. Pitarka (2004). Broadband time history simulation using a hybrid approach, *Proc. 13th World Conference on Earthquake Engineering*, Vancouver, Canada. paper no. 1098.

Graves, R.W., P. Somerville, N. Collins, A. Pitarka and S. Ni (2007). Analysis of strong ground motions from the June 12, 2005 Anza earthquake. Report to CSMIP Data Interpretation Project, California Geological Survey.

Hartzell, S., C. Langer and C. Mendoza (1994). Rupture histories of eastern North American earthquakes. *Bull. Seism. Soc. Am.* 84, 1703-1724.

Johnston, A.C. (1996). Seismic moment assessment of earthquakes in stable continental regions: III. New Madrid 1811-1812, Charleston 1886 and Lisbon 1755, Geophys. J. Int. 126, 314-344.

Leonard, M (2008). Earthquake fault scaling: relating rupture length, width, average displacement and seismic moment release. Manuscript prepared for BSSA.

Liang, J. Z., Hao, H., Gaull, B. A. and Sinadinovski, C. (2008). Estimation of Strong Ground Motions in Southwest Western Australia with a Combined Green's Function and Stochastic Approach', Journal of Earthquake Engineering, 12:3,382 – 405.

Petersen, M., A. Frankel, A., S. Harmsen, C. Mueller, K. Haller, R. Wheeler, R. Wesson, Y. Zeng, O. Boyd, D. Perkins, N. Luco, E. Field, C. Wills, and K. Rukstales (2008). Documentation for the 2008 updated of the United States National Seismic Hazard Maps. *U.S. Geological Survey Open File Report* 2008-1128.

Risk Engineering, Inc. (2001). Technical Basis for Revision of Regulatory Guidance on Design Ground Motions: Hazard- and Risk-consistent Ground Motion Spectra Guidelines. *NUREG/CR-6728*.

Somerville, P., R.W. Graves, N.F. Collins, S.G. Song, and S. Ni (2009). Ground motion models for Australian earthquakes. Report to Geoscience Australia, 29 June 2009.

Somerville, P.G., N. Collins, N. Abrahamson, R. Graves and C. Saikia (2001). Earthquake source scaling and ground motion attenuation relations for the central and eastern United States. Final Report to the U.S. Geological Survey, Contract No. 99HQGR0098.

Somerville, P.G., K. Irikura, R. Graves, S. Sawada, D. Wald, N. Abrahamson, Y. Iwasaki, T. Kagawa, N. Smith and A. Kowada (1999). Characterizing earthquake slip models for the prediction of strong ground motion. *Seismological Research Letters*, 70, 59-80.

Somerville, P.G., J.P. McLaren, L.V. LeFevre, R.W. Burger and D.V. Helmberger (1987). Comparison of source scaling relations of eastern and western North American earthquakes, *Bull. Seism. Soc. Am*., **77**, 332-346.

Toro, G.R., N.A. Abrahamson, and J.F. Schneider (1997). Model of strong ground motions from earthquakes in central and eastern North America: best estimates and uncertainties. *Seismological Research Letters*, 68(1), 41-57.